



## Discover Generics

Cost-Effective CT & MRI Contrast Agents



FRESENIUS  
KABI

WATCH VIDEO

# AJNR

## MR Spectroscopy-Aided Differentiation: "Giant" Extra-Axial Tuberculoma Masquerading as Meningioma

P.C. Khanna, S. Godinho, D.P. Patkar, S.A. Pungavkar and  
M.A. Lawande

This information is current as  
of June 28, 2025.

*AJNR Am J Neuroradiol* 2006, 27 (7) 1438-1440  
<http://www.ajnr.org/content/27/7/1438>

## CASE REPORT

P.C. Khanna  
S. Godinho  
D.P. Patkar  
S.A. Pungavkar  
M.A. Lawande

# MR Spectroscopy-Aided Differentiation: "Giant" Extra-Axial Tuberculoma Masquerading as Meningioma

**SUMMARY:** Tuberculosis is common in the developing world and in developed nations secondary to increasing immunocompromise in the population. It commonly causes meningitis and parenchymal tuberculomas. We present a case of an unusual masslike "giant" extra-axial tuberculoma during pregnancy. Unusual morphology and size at imaging made meningioma a close differential. MR spectroscopy served to complement MR imaging, providing diagnostic confirmation and depicted findings characteristic of a tuberculoma.

**T**uberculosis, an important public health problem compounded by the upsurge of the human immunodeficiency virus usually results from *Mycobacterium tuberculosis* infection, though *Mycobacterium bovis*, a frequent pathogen of the past, and *Mycobacterium avium* complex (*M avium* and *M intracellulare*) are infrequently encountered. Central nervous system (CNS) tuberculomas typically result from hematogenous dissemination and, upon histologic examination, are granulomas with central caseous necrosis.

Although intra-axial tuberculous granulomata are the more common variety, extra-axial lesions are rarely encountered<sup>1-6</sup> and may present diagnostic dilemmas that need to be resolved by imaging and allied techniques, so as to circumvent unnecessary chemotherapy, biopsies, and surgery. MR spectroscopy is one such technique that we used.

## Case Report

A 25-year-old pregnant patient (gravida 1, para 0) presented at 27 weeks' gestation with severe headaches and focal right-sided convulsions of 3 months' duration without fever, papilledema, or elevated blood pressure. Elevated erythrocyte sedimentation rate (ESR) was noted. Postpartum lumbar puncture and CSF analysis after imaging studies revealed mild lymphocytic predominance and positive polymerase chain reaction (PCR) for tuberculosis. Antituberculous therapy was begun after suspending breast-feeding.

Two MR examinations (1.5T EchoSpeed; GE Medical Systems, Milwaukee, Wis) obtained at 27 weeks and postpartum revealed an unchanged 3.8 × 2.75 × 3.0-cm left frontal extraparenchymal mass lesion that appeared hypointense on T1-weighted images (T1WI; Fig 1A), with a thick, isohypointense rim. On T2-weighted images (T2WI, Fig 1B) and fluid-attenuated inversion recovery (FLAIR), it appeared predominantly hypointense with central hyperintensity, consistent with necrosis. The lesion appeared dark on diffusion-weighted images (DWI; Fig 2A). Contrast (gadolinium-diethylenetriaminepentaacetic acid [Gd-DTPA]) enhanced MR (Fig 2B) depicted prominent heterogeneous central enhancement with a thick, peripheral nonenhancing wall and peripheral rim-enhancement. Adjoining meningeal enhancement ("dural tail"), adjacent CSF cleft, mass-effect, and vasogenic edema were noted. MR angiography and venography revealed no abnormal vascularity or occlusion. MR perfusion revealed no changes in cerebral blood volume or flow. A dif-

ferential diagnosis of inflammatory granuloma (with leptomeningitis and cerebritis) versus meningioma was considered.

A volume of interest of 8.0 mL was selected from the center of the lesion on T2WI and image-guided, single-voxel, point-resolved MR spectroscopy (PRESS; repetition time [TR]/echo time [TE] = 1500ms/35ms) was used, because with this technique, lipid contamination in volumes abutting fat structures is negligible. Multivoxel MR spectroscopy was obtained as well. Findings were consistent with necrotic inflammatory granuloma/tuberculoma, revealing elevated lipid-lactate and choline (Cho) peaks with barely detectable *N*-acetylaspartate (NAA) and creatine (Cr). No abnormal peak was detected corresponding to alanine. Follow-up MR spectroscopy (Fig 3A,B) remained unchanged. Long TE (144 ms; Fig 3B) MR spectroscopy sequence obtained from an identical location did not suppress the 1.33-ppm peak, confirming predominance of lipid. Findings were more conspicuous with multivoxel spectroscopy.

Based on imaging, spectroscopic, and clinical features, a diagnosis of giant extra-axial tuberculoma was made. Surgical excision biopsy confirmed the diagnosis.

## Discussion

Although intraparenchymal tuberculomas are common, solid extra-axial tuberculous masses are *extremely* uncommon.<sup>1</sup> We believe our case is unique in that our patient was pregnant and immunocompetent, MR findings mimicked those of a similarly located isolated meningioma, and we were able to successfully use spectroscopy to confirm our diagnosis.

Extra-axial tuberculomas simulating meningiomas may be located in the frontoparietal areas<sup>2</sup> and pontine, pericallosal,<sup>4</sup> and suprasellar cisterns. Cystic<sup>1</sup> and en-plaque meningioma<sup>5</sup> mimics and those caused by *M avium* (noted in patients with systemic lupus erythematosus<sup>3</sup>) can be encountered. Most appear hypointense to isointense to gray matter<sup>1-6</sup> on T1WI and T2WI and variable on DWI, often with a hyperintense rim; those with hyperintense centers on T2WI are usually hyperintense on DWI.<sup>7</sup> Meningiomas typically appear isointense to gray matter on T1WI and T2WI and DWI, unless atypical or aggressive.<sup>8</sup> Signal intensity is a function of intralosomal lipids, macrophages, fibrosis, and cellular infiltrates.<sup>9</sup>

In vivo proton MR spectroscopy has been studied extensively in this context. Tuberculomas are characterized by a prominent decrease in NAA/Cr and slight decrease in NAA/Cho.<sup>10</sup> Lipid-lactate peaks are usually elevated (86% of tuberculomas<sup>11</sup>). Paradoxically, lipid/Cr may occasionally be *decreased* relative to normal cerebral parenchyma, probably resulting from small dimensions of most tuberculomas rela-

Received July 11, 2005; accepted after revision August 31.

From the Department of Magnetic Resonance Imaging, Nanavati Hospital, Mumbai, India.

Address correspondence to Paritosh C. Khanna, 2200 Columbia Pike, Apt # 418, Arlington, VA 22204; e-mail: paritoshkhanna@hotmail.com

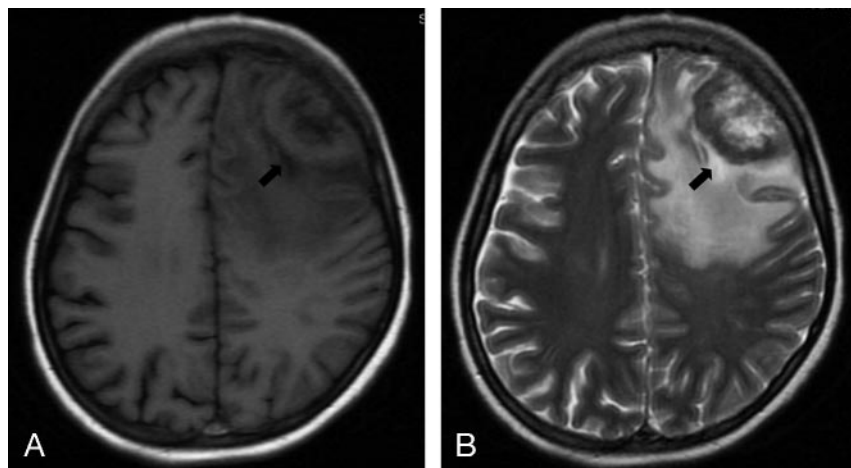


**Fig 1.** Axial T1WI (A; fast spin echo; TR/TE = 2015ms/9.7ms) and T2WI (B; fast spin echo; TR/TE = 4360ms/83ms) depicting a lobulated, dura-based lesion in the left frontal convexity that is predominantly hypointense on T1WI with a thick, iso-hypointense rim. On T2WI, it is of mixed intensity but predominantly hypointense with a hyperintense center. Displacement of the underlying parenchyma and a CSF cleft are identified (arrows). A large component of vasogenic edema is visualized.

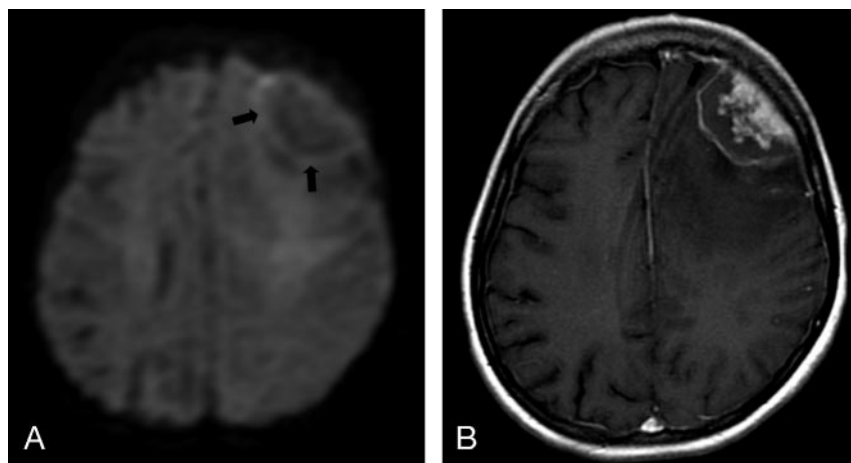


**Fig 2.** Axial DWI (A; TR/TE = 3000ms/11ms) depicts a dark-appearing lesion, with a hyperintense rim (arrows). Axial contrast-enhanced T1WI (B; Gd-DTPA enhanced fast spin echo; TR/TE = 2015ms/9.7ms) depicts prominent central enhancement, a thick peripheral nonenhancing component and rim-enhancement beyond this. There is thick enhancement of adjoining meninges ("dural-tail" sign, arrow) with mild enhancement of meninges in the anterior interhemispheric region and the right cerebral convexity (not shown).

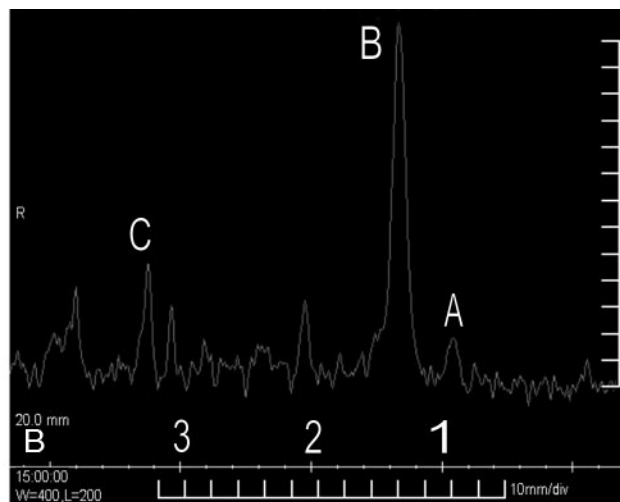
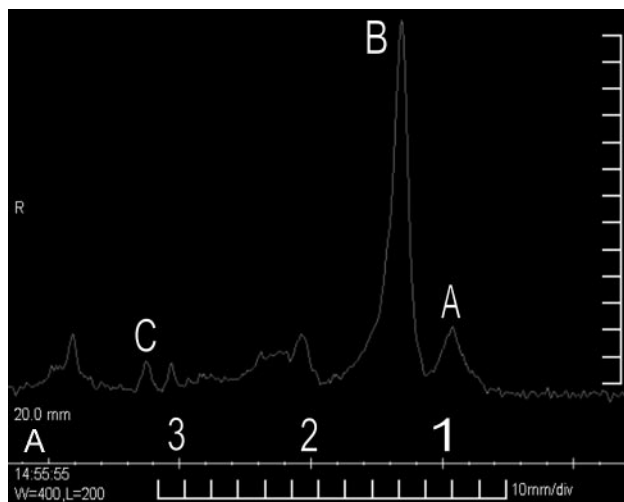


**Fig 3.** Single-voxel PRESS MR spectroscopy (A; TR/TE = 1500ms/35ms). Adequate water suppression has been achieved. Reading from right to left, peaks A and B (tall and broad) at 0.9 and 1.33 ppm, respectively, represent typical long-chain lipids (lipid/lactate). NAA and Cr are barely detectable. A small Cho peak, C, is seen to resonate at 3.2 ppm. Long TE MR spectroscopy (B; TR/TE = 1500ms/144ms) depicts persistence of predominant lipid peak at 1.33 ppm.

tive to voxel volume. 3D multivoxel proton spectroscopy with 2D chemical shift imaging interrogates relatively small voxel volumes and overcomes this paradox.<sup>12</sup> Meningiomas invariably have elevated alanine. A high lipid/Cr ratio may also be noted.<sup>10</sup> "Finger-printing" of *M tuberculosis* cell-wall biochemicals in tuberculomas is now possible, facilitating their detection.<sup>13</sup> T1-weighted magnetization transfer MR imaging

is a useful adjunct to MR spectroscopy and shows promise in tissue characterization of CNS tuberculomas.<sup>13</sup>

### Conclusions

When diagnostic dilemmas present themselves, MR spectroscopy considered in perspective with MR imaging and clinicopathologic features can be useful in certain situations. Rare as

they are, extra-axial tuberculomas may masquerade as meningiomas. To our knowledge, ours is the first report of an extra-axial “giant” tuberculoma that bore a striking resemblance to meningioma and in which diagnostic confirmation was obtained using proton MR spectroscopy that was later corroborated by surgical biopsy and histopathology.

## References

1. Shindo A, Honda C, Baba Y. A case of an intracranial tuberculoma, mimicking meningioma that developed during treatment with anti-tuberculous agents. *No Shinkei Geka* 1999;27:837–41
2. Isenmann S, Zimmermann DR, Wichmann W, et al. Tuberculoma mimicking meningioma of the falx cerebri. PCR diagnosis of mycobacterial DNA from formalin-fixed tissue. *Clin Neuropathol* 1996;15:155–58
3. Di Patre PL, Radziszewski W, Martin NA, et al. A meningioma-mimicking tumor caused by *Mycobacterium avium* complex in an immunocompromised patient. *Am J Surg Pathol* 2000;24:136–39
4. Adachi K, Yoshida K, Tomita H, et al. Tuberculoma mimicking falx meningioma—case report. *Neurol Med Chir (Tokyo)* 2004;44:489–92
5. Bauer J, Johnson RF, Levy JM, et al. Tuberculoma presenting as an en plaque meningioma. Case report. *J Neurosurg* 1996;85:685–88
6. Lindner A, Schneider C, Hofmann E, et al. Isolated meningeal tuberculoma mimicking meningioma: case report. *Surg Neurol* 1995;43:81–84
7. Batra A, Tripathi RP. Diffusion-weighted magnetic resonance imaging and magnetic resonance spectroscopy in the evaluation of focal cerebral tubercular lesions. *Acta Radiol* 2004;45:679–88
8. Filippi CG, Edgar MA, Ulug AM, et al. Appearance of meningiomas on diffusion-weighted images: correlating diffusion constants with histopathologic findings. *AJNR Am J Neuroradiol* 2001;22:65–72
9. Gupta RK, Pandey R, Khan EM, et al. Intracranial tuberculomas: MRI signal intensity correlation with histopathology and localised proton spectroscopy. *Magn Reson Imaging* 1993;11:443–49
10. Bulakbasi N, Kocaoglu M, Ors F, et al. Combination of single-voxel proton MR spectroscopy and apparent diffusion coefficient calculation in the evaluation of common brain tumors. *AJNR Am J Neuroradiol* 2003;24:225–33
11. Pretell EJ, Martinot C Jr., Garcia HH, et al. Cysticercosis working group in Peru. Differential diagnosis between cerebral tuberculosis and neurocysticercosis by magnetic resonance spectroscopy. *J Comput Assist Tomogr* 2005;29:112–14
12. Gonen O, Murdoch JB, Stoyanova R, et al. 3D multivoxel proton spectroscopy of human brain using a hybrid of 8th-order Hadamard encoding with 2D chemical shift imaging. *Magn Reson Med* 1998;39:34–40
13. Gupta RK, Husain M, Vatsal DK, et al. Comparative evaluation of magnetization transfer MR imaging and in-vivo proton MR spectroscopy in brain tuberculomas. *Magn Reson Imaging* 2002;20:375–81